

Optimization of Phase-Engineered a-Si:H- Based Multijunction Solar Cells

**C. R. Wronski, R. W. Collins,
J. Deng, J. Pearce, V. Vlahos, M. Albert, G. M. Ferreira, C. Chen**

**Center for Thin Film Devices
The Pennsylvania State University
University Park, PA 16802**

**Quarterly Technical Status Report
January 2004 – April 2004**

Subcontract No. NDJ-1-30630-01

NREL Technical Monitor: Bolko von Roedern

Table of Contents

Table of Contents	2
Executive Summary	3
Task 1: Materials Research and Device Development	3
Figure 1.1	3
Task 3: Device Loss Mechanisms.....	3
Task 4: Characterization Strategies for Advanced Materials	4
Task 3: Device loss mechanisms	5
Microcrystalline p-contact in a-Si:H n-i-p solar cells.....	5
Determination of Mobility Gap with J_D -V characteristics.....	5
Figure 3.1	6
Task 4: Characterization Strategies for Advanced Materials	8
Evolution of D^0 and non- D^0 Light Induced Defect States in a-Si:H Materials	8
Appendix A	13

Executive Summary

Task 1: Materials Research and Device Development

Real Time Spectroscopic Ellipsometry (RTSE) studies on the deposition of amorphous silicon germanium alloys for high performance solar cells are being carried out. In these studies the process parameters including different silane/germane and hydrogen dilution ratios (R) are being investigated. For the *first time* RTSE results have been obtained on the micro-structural evolution of SiGe:H alloys. This is illustrated with the results in Figure 1.1 for a film deposited with RF-PECVD at 200°C with low power and low pressure. In this case the silane/germane ratio was 5:1, and hydrogen/silane dilution 40 the deposition rate was 0.6Å/s. In Figure 1.1 an amorphous to amorphous transition can be seen at 220Å with no evolution into protocrystalline growth. It can be noted that, under similar deposition conditions for Si:H with hydrogen/silane dilution ratio of 40, protocrystalline growth is present with a transition to a mixed amorphous/microcrystalline phase at around this thickness. This clearly illustrates the large differences in growth that have to be characterized in detail in order to *systematically* optimize the alloy materials and their solar cell structures.

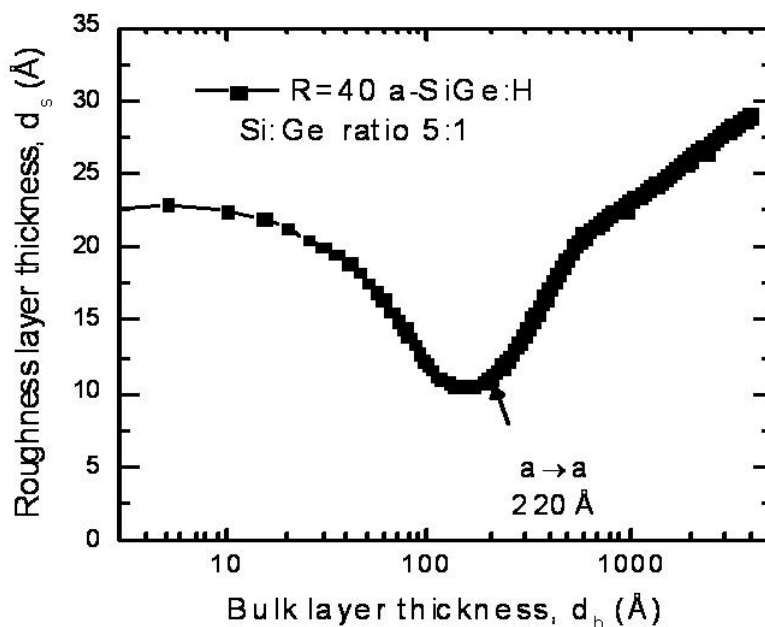


Figure 1.1: Roughness evolution with bulk layer thickness for a R=40 a-SiGe:H i-layer.

Task 3: Device Loss Mechanisms

The studies on a-Si:H solar cells have continued to address the mechanisms and defect states determining their characteristics using the powerful and sensitive techniques based on J_D -

V characteristics. The self-consistent interpretation of a wide range of these characteristics is being carried out with the model previously described¹. It has been confirmed that as predicted by the model the contribution of p/i recombination to J_D -V characteristics is in the form of constant diode quality factor n equal to 1. This has been demonstrated with truly microcrystalline Si:H p-contacts with 1 sun V_{OC} values of around 0.55V, similar to those reported for microcrystalline/nanocrystalline cells. These results also *bring to closure* the issue of microcrystalline versus protocrystalline p-Si:H contacts for high V_{OC} on a-Si:H solar cells since the latter yield 0.92V.

The “differential diode quality factors”, $n(V)$ resulting from bulk recombination in the i-layers are being further characterized in order to obtain information about the distributions of gap states in different i-layer materials and their evolution during light and forward bias induced degradation (see Appendix A). Because the “effective diode quality factor” reported for microcrystalline/nanocrystalline cells are similar to those in a-Si:H cells studies will be carried out on the J_D -V characteristics of such cells provided by United Solar Ovonic. De-convolution of the gap state distributions and densities of the intrinsic as well as light induced defects in a-Si:H from J_D -V characteristics has been undertaken.

A new and accurate method for evaluating the mobility gap of a-Si:H i-layers has been developed which takes into account the presence of bias dependent $n(V)$. This method, which eliminates the uncertainties associated with the extrapolations of J_D -V to $V=0$ yields mobility gap values with an accuracy of ± 10 meV. It also offers a more reliable approach to characterizing the bandgaps in microcrystalline/nanocrystalline cells, particularly if they also exhibit bias dependent “differential diode quality factors” $n(V)$.

Task 4: Characterization Strategies for Advanced Materials

Studies are continuing on the evolution of light induced defects in protocrystalline (diluted) a-Si:H films under 1 sun illumination. A room temperature reversal is observed in the photocurrents at 25°C, which is consistent with the relaxation in the recombination currents on corresponding p-i-n solar cells. It is consistent with the presence of “fast” states such as have been observed after high intensity illumination. Even with the limitations imposed by the relaxation in the light induced changes on the subgap absorption measurements, the evolution of distinctly different gap states centered around 0.9 and 1.15eV from the conduction band was identified. The evolution of the electron occupied states, $kN(E)$, at these two energies has been compared with that of the neutral dangling bond (D^0) densities as measured with electron spin resonance at the University of Utah. Because of the similarity between the preliminary results of the respective kinetics it has not been possible to identify which states correspond to the D^0 nor to draw any reliable conclusions about the nature of the different states. Further investigation of the evolution of the defect states in these protocrystalline a-Si:H will be carried out in collaboration with the University of Utah and P. Stradins at NREL. In parallel detailed studies on corresponding p-i-n solar cells will be continued.

¹ Penn State 2003 NREL Final Report

Task 3: Device loss mechanisms

Microcrystalline p-contact in a-Si:H n-i-p solar cells

It has been well established in the previous reports that the interface recombination dominated currents can be identified through its nearly constant value of effective diode quality factor n , which is very close to 1. Applying this criterion to the case of a n-i-p cell with microcrystalline p-layer, conclusion is readily reached that due to the incorporation of this p-layer the dark currents in this cell are p/i interface recombination (or thermal emission) dominated. Shown in Figure 3.1 are the J_D -V characteristics for a p (SiC:H) -i-n cell and a n-i-p (μ c-Si) cell. The bulk of both cells consist of 0.4 μ m thick R=10 i-layer. It can be seen in the figure that not only the current is much higher in n-i-p cell than that in p-i-n cell but also the slope of the J_D -V characteristics in n-i-p cell is much steeper, which indicates a smaller value of n . This is even more clearly seen for the corresponding $n(V)$ characteristics as shown in Figure 3.2. It can be seen that most of the values of $n(V)$ for the p-i-n cell are larger than 1.4, while for the n-i-p cell the values of $n(V)$ are very close to 1 for most of the exponential region in its J_D -V characteristics before the current becomes injection limited. These results clearly point to a fact that due to small band-gap of the μ c-Si p-layer, the built-in potential V_{bi} across the cell is so low that the electron concentration is very high at p/i interface which results in an interface recombination or thermal emission rate much larger than that occurring in the i-layer. This high recombination rate is further confirmed with the result on 1 sun V_{OC} , which has a value as low as 0.55V compared to 0.92V for the p-i-n cell. The low value of V_{bi} due to the μ c-Si p-layer is also consistent with the relative low value of fill factor of 0.67 as compared to 0.73 for the p-i-n cell. This further confirms that the incorporation of truly μ c-Si p-layer into the a-Si:H solar cell only degrades the cell performance and the validity of the model for operation of a-Si:H solar cells based on first principles².

Determination of Mobility Gap with J_D -V characteristics

J_D -V characteristics have been used to evaluate the mobility gaps of a-Si:H i-layers³ based on the dark currents having the following form:

$$J_R = J_0 \exp\left(\frac{qV}{nkT}\right) \quad (1)$$

with

$$J_0 = J_{00} \exp\left(\frac{-E_A}{2kT}\right) \quad (2)$$

² J. Deng, J.M. Pearce, R.J. Koval, V. Vlahos, R.W. Collins, and C.R. Wronski, *Appl. Phys. Lett.* **82**, 3023 (2003).

³ M.S. Bennett and R.R. Arya, *Solar Cells*, **18**, 289 (1986).

where E_A is approximately equal to the mobility gap. It has also been suggested that J_{00} has a temperature dependence of the form of T^3 . A fitting to the plot of J_0/T^3 versus $1/T$ has then been used to determine the mobility gap. However, due to the continuous gap state distribution the J_D - V characteristics do not exhibit an exact exponential form as given by Eqn. 2 and the dark currents have the following form:

$$J_R = f(V)T^3 \exp\left(\frac{qV - E_A}{2kT}\right) \quad (3)$$

Consequently, J_0 as defined in Eqn. 1 is no longer independent of V so that J_0 cannot be used as an *accurate* method for determining the mobility gap. On the other hand, according to Eqn. 3 through a fitting of the plots of $J_R/(T^3 \cdot \exp(qV/2kT))$ versus $1/T$, the mobility gap can be obtained for any arbitrarily selected voltage as long as the current is still dominated by bulk recombination. Shown in Figure 3.3 are the results obtained on the p-i-n cell of Figure 3.1. Three bias levels, 0.5, 0.6 and 0.7V were chosen to perform the fitting. It can be seen that excellent fits obtained with these three biases yield a mobility gap of 1.77eV for the R=10 i-layer with an error smaller than 10meV.

This new and accurate method can be very useful in studying i-layer properties. For instance, it can be used to probe the mobility gap profile in microcrystalline i-layer of n-i-p solar cells where the doping in p and n contacts are different and there is an evolution in the crystalline phase of the i-layer.

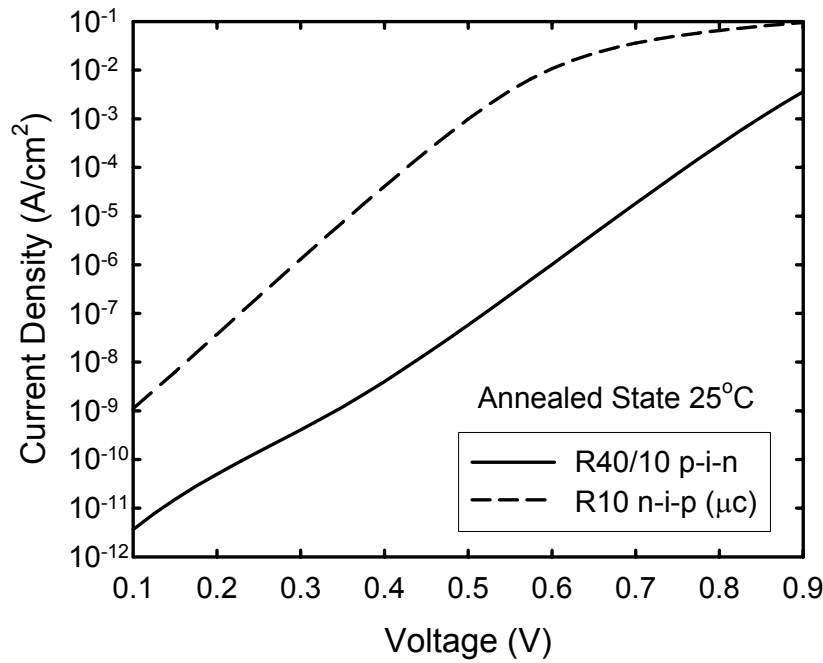


Figure 3.1: J_D - V characteristics of a p-i-n cell with R=10 i-layer, R=40 p/i interface layer and a n-i-p cell with μc -p layer.

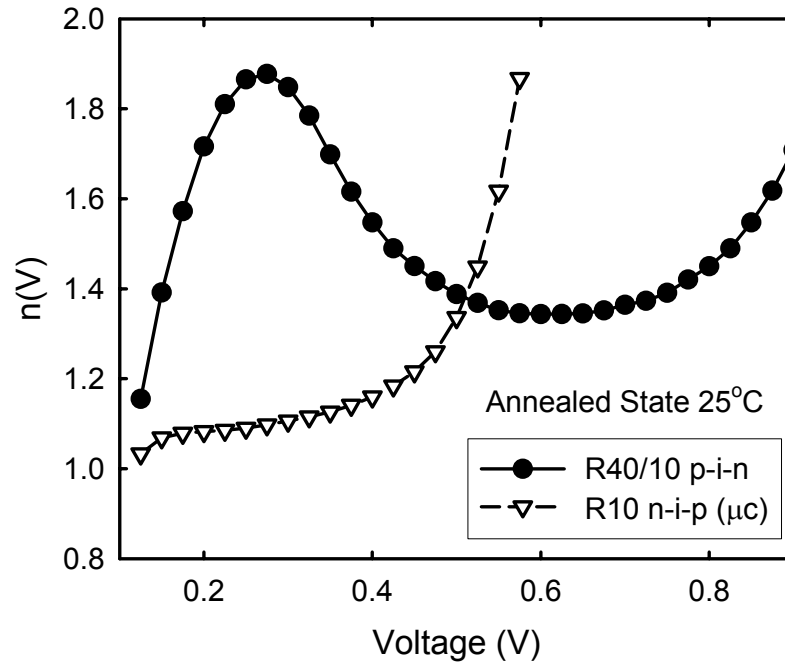


Figure 3.2: $n(V)$ characteristics for the cells of Figure 3.1.

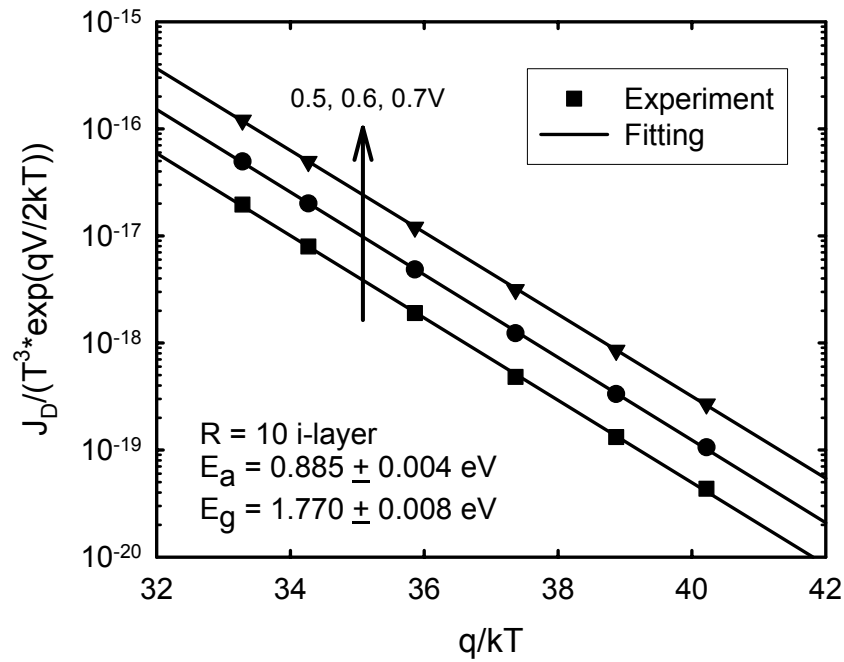


Figure 3.3: Numerical fitting of the activation energy of the J_D -V characteristics for the p-i-n of Figure 3.1.

Task 4: Characterization Strategies for Advanced Materials

Evolution of D^0 and non- D^0 Light Induced Defect States in a-Si:H Materials

Recently the evolution of two distinctly different light induced defect states around and below midgap was identified from the comparison of changes in subgap absorption spectra obtained for a-Si:H films with a large difference in their microstructure^{4,5}. This was obtained by analyzing the spectra not just in terms of a single defect state, as is generally done, but by taking into account the presence of multiple defect states. To further characterize these light induced gap states a study was undertaken on protocrystalline (diluted) a-Si:H that exhibits “superior” stability and reaches a degraded steady state under 1 sun illumination in < 100 hours.

Although large changes in photo-conductivities after 1 sun illumination indicative of “fast” states have been observed⁶ there were no results reported indicative of their subsequent annealing at room temperature. Very recently, however, we observed in protocrystalline cell structures after 1 sun illumination at 25°C large relaxation in their forward bias currents that correspond to the recombination in the bulk i-layers as discussed in Task 3. This direct evidence for such room temperature annealing, which could be directly observed in the presence of small quasi-Fermi level splitting, triggered a careful investigation of the light induced changes in corresponding i-layer films. Similar relaxation is observed in the photocurrents having small quasi-Fermi level splitting and correspondingly low carrier recombination. It should be pointed out here, that although the relaxation was observed in films with co-planer configurations in air where surface water/contaminant adsorption and desorption could shift the Fermi level, the room temperature annealing effect was established by correlating the relaxation with the results on cells. The solar cells were completed structures with 1000Å of Cr top contacts and would not have been affected by adsorption and desorption of water/contaminants. In addition, the initial rapid changes in the photoconductivity, which also could be due to absorption/desorption, were found to be authentic when checked with uv exposure and under vacuum. This newly observed phenomenon of annealing in the light induced changes in films, which occurs not only after 1 sun illumination but also at room temperature, complicates the reliable correlation of results from different measurements. This was taken into account in the study reported here in which preliminary comparisons are made between the light induced changes in photocurrents, the electron occupied states obtained from subgap absorption measurements using dual beam photoconductivity (DBP), and the densities of D^0 states measured with ESR.

The protocrystalline a-Si:H materials with a bandgap of ~1.8eV, were deposited using hydrogen dilution of silane ratio of 10 by plasma enhanced chemical vapor deposition as described previously⁷. The 0.8µm films were deposited onto n+ contacts on 7059 glass in order to establish Ohmic behavior in photocurrents over a wide voltage range even in the annealed state (AS). Photocurrents were measured with volume absorbed light from an ENH lamp with a

⁴ J. M. Pearce, J. Deng, R. W. Collins, and C. R. Wronski, *Appl. Phys. Lett.*, **83**(18), pp. 3725-3727 (2003).

⁵ J. M. Pearce, J. Deng, V. Vlahos, R. W. Collins, and C. R. Wronski, “Light Induced Changes in Two Distinct Defect States At and Below Midgap in a-Si:H”, *Proceedings of the 3rd World Conference on Photovoltaic Energy*, 50-D14-01, (2003).

⁶ L. Jiao, H. Liu, S. Semoushikina, Y. Lee, C. R. Wronski, *Appl. Phys. Lett.* **69**, p.3713 (1996).

⁷ C. R. Wronski, R. W. Collins, V. Vlahos, J. M. Pearce, J. Deng, M. Albert, G. M. Ferreira, and C. Chen, “Optimization of Phase-Engineered a-Si:H-Based Multijunction Solar Cells”, *National Renewable Energy Laboratory Annual Report*, Contract #: NDJ-2-30630-01, (2004).

narrow band pass filter at $\lambda=687\text{nm}$. The kinetics of the light induced changes were characterized with a generation rate (G) of $5 \times 10^{15} \text{cm}^{-3} \text{s}^{-1}$ - the bias illumination used in DBP measurements in the AS. This G is equivalent to the electron quasi-Fermi level around 0.7eV from the conduction band edge and estimated split of $\sim 0.4\text{eV}$ between the quasi-Fermi levels. The subgap absorption measurements were carried out on a new DBP apparatus described in detail in our last annual report. This system allowed the reliable range of the $\alpha(E)$ spectra to be obtained up to 0.7eV from the conduction band. It also offered high resolution (0.01eV), high signal to noise ratio and improved the acquisition times for the spectra to be consistently under 30 minutes. In the study on the evolution of defect states attention was given to maintaining the same quasi-Fermi level splitting in the measurements of $\alpha(h\nu)$ before and during the degradation to ensure that the region in the gap over which states act as recombination centers remains constant. Absence of this in the occupation of the gap states, particularly near midgap, introduces variables other than the evolution of the light induced defects. As a consequence AS generation rate of $5 \times 10^{15} \text{cm}^{-3} \text{s}^{-1}$ was increased to $\sim 10^{17} \text{cm}^{-3} \text{s}^{-1}$ after 100 hours of 1 sun illumination. The method developed by Wiedeman, Bennett and Newton was utilized for removing the interference fringes in $\alpha(h\nu)$ spectra⁸. The values of the electron occupied density of states were derived using the analysis previously described where the values of k, which depend on the dipole matrix elements for transitions from localized to extended states, were assumed to be constant.

Electron spin resonance experiments were conducted with a Bruker Instruments ESR spectrometer with samples deposited on quartz substrates utilizing the first harmonic detection technique previously described⁹. The measurements were carried out several days after light soaking. However, insights relevant to the $kN(E)$ spectra were obtained because the absence of long term relaxation in ESR spin densities has been reported¹⁰.

Recovery in photocurrents was observed at room temperature immediately after 1 sun illumination at carrier generation rates $< 10^{16} \text{cm}^{-3} \text{s}^{-1}$. This was observed after all light soaking times and is as illustrated in Fig. 4.1, where the photocurrents with $G = 10^{15} \text{cm}^{-3} \text{s}^{-1}$ are shown immediately after light soaking, 20 minutes and after 1 hour of recovery. It can be clearly seen that the kinetics that are measured are dramatically effected by the time after exposure to 1 sun illumination. It can also be seen that as the light soaking time increases the recovery rate relative to the initial values decreases and slows down considerably after the first hour. The rate of recovery in the photocurrents decreased as the G increased as the quasi-Fermi level splitting and carrier recombination increased. This can be seen more clearly in Fig. 4.2, where the normalized photocurrent as a function of relaxation time is shown for a R=10 film degraded under 1 sun illumination at 25°C for 1minute, 2hours, and 24 hours. This is in agreement with the results on cells. It can also be pointed out that exposure to high G (e.g. 1 sun illumination) rapidly *erases* the recoveries in less than 1 minute. These results are indicative of the presence of the “fast” and “slow” states previously observed in the recovery of the FF after high intensity illumination of cells^{11,12} and 1 sun degradation kinetics of cells and films¹³. As discussed earlier this relaxation in the light induced changes complicates the characterization of the light induced gap states with

⁸ S. Wiedeman, M. S. Bennett, and J. L. Newton, *Mater. Res. Soc. Symp. Proc.* **95**, pp. 145-150 (1987).

⁹ 16. B. Yan and P. C. Taylor, *Mat. Res. Soc. Symp. Proc.* **507**, 805 (1998).

¹⁰ 17. P.C. Taylor and W. D. Ohlsen, *Solar Cells*, **9** pp. 113-118 (1983).

¹¹ L. Yang, L. Chen, and A. Catalano, *Appl. Phys. Lett.* **59**, p. 840 (1991).

¹² X. Xu, J. Yang, and S. Guha, *Mat. Res. Soc. Proc.*, **297** 649 (1993).

¹³ J. M. Pearce, R. J. Koval, X. Niu, S. J. May, R.W. Collins, and C. R. Wronski, , *17th European Photovoltaic Solar Energy Conference Proceedings*, 3, pp. 2842-2845 (2002).

subgap absorption measurements because as the fast states anneal out different gap state distributions would be measured at different times after light soaking.

Although the effects of relaxation were taken into account on the measurement of subgap absorption, several complexities exist from the experimental limitations imposed on the time, approximately 20 minutes taken to scan the full spectra. The acquisition of the $\alpha(h\nu)$ spectra begins at the high photon energies (1.65eV) so that during the course of the measurement the defect states at the lower energies ($\sim < 1.0\text{eV}$) have time to relax. Consequently the $\alpha(h\nu)$ results obtained immediately after the 1 sun illumination include the effects of relaxation on the spectra. Subgap spectra were taken immediately and 30 minutes after the light soaking. Relaxation was observed in the $\alpha(E)$ spectra. Thus to minimize the effects of the relaxation, which is fastest in the first 30 minutes, the $\alpha(h\nu)$ results that were initiated 30 minutes after 1 sun illumination (the second scan) are shown as $kN(E)$ spectra in Fig. 4.3. The $kN(E)$ spectra, derived from previously reported analysis¹⁴ is given by $(h\nu)d[\alpha(h\nu)]/dE - \alpha(h\nu)$, are shown in Fig. 4.3 as a function of energy from the conduction band (E_C) in the AS and after 1 sun illumination at 25°C for 5 minutes, 30 minutes, 1 hour, 10 hours, 24 hours, and 100 hours. It should be noted that in these results of $kN(E)$ are dominated by the $(h\nu)d[\alpha(h\nu)]/dE$ term and not the magnitude of $\alpha(h\nu)$. The drop off in $kN(E)$ for all the soaking times $\sim 0.2\text{eV}$ above midgap can be attributed to the position of the electron quasi-Fermi level above which no states are occupied by electrons. The striking feature of the results in Fig. 4.3 is the very large change in the $kN(E)$ spectra that occur in the first half hour. Such large changes have not been observed in the results on corresponding solar cells. Although significant changes in $\alpha(h\nu)$ spectra have been reported for protocrystalline a-Si:H the extent of the changes in the gap states themselves were not evaluated. Clear evolution of light induced gap states centered at 0.9eV and 1.15eV are seen in Fig. 4.3. The rapid increases of the occupied defect states centered at midgap can be attributed to the low densities of these states in the AS. The defect states centered around 1.15eV, which are close to the valence band tail states and thus contain a greater error, still exhibit a clearly identifiable evolution.

¹⁴ J. M. Pearce, J. Deng, R. W. Collins, and C. R. Wronski, *Appl. Phys. Lett.*, **83**(18), pp. 3725-3727 (2003).

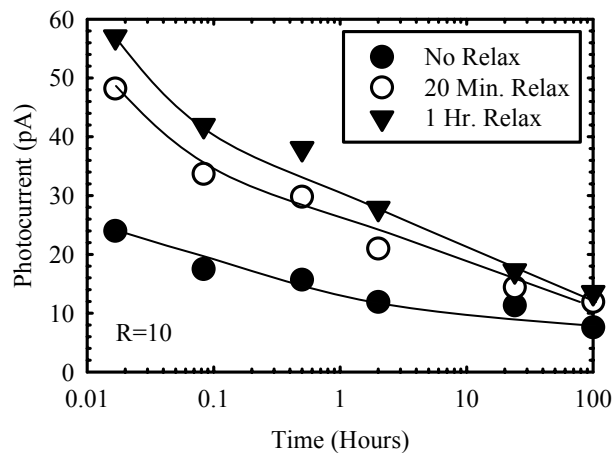


Fig. 4.1 The photocurrent with $G = 5 \times 10^{15} \text{ cm}^{-3} \text{ s}^{-1}$ as a function of 1 sun illumination time immediately after light soaking, and after 20 minutes and 1 hour of recovery.

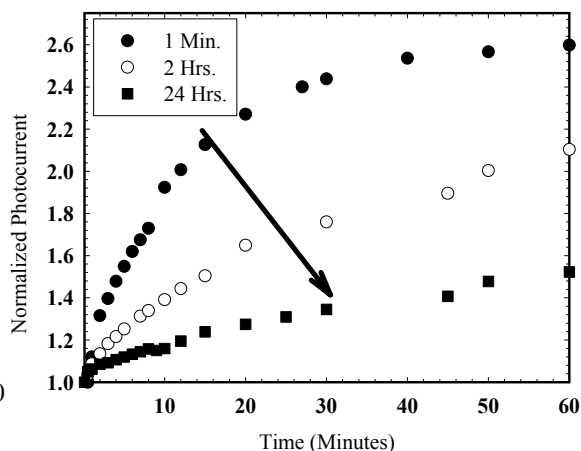


Fig. 4.2 Normalized photocurrent vs. room temperature relaxation time in minutes after 1 minute, 2 hours, and 24 hours of 1 sun illumination.

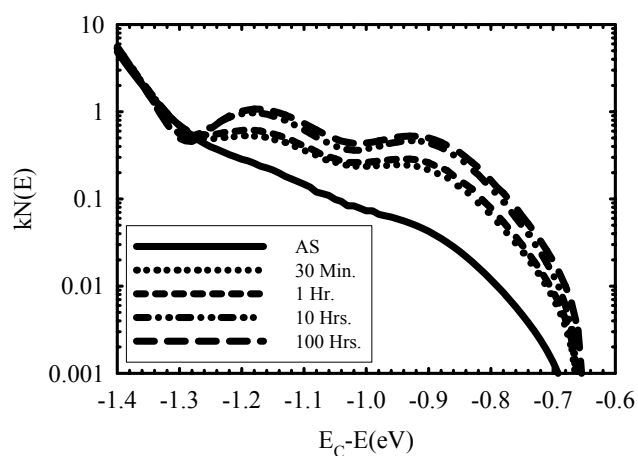


Fig. 4.3. Evolution in the electron occupied gap state density $kN(E)$ as a function of energy from the conduction band (E_C).

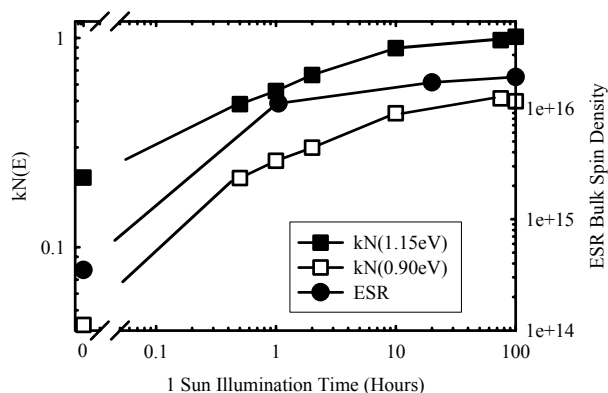


Fig. 4.4 $kN(E)$ at 0.9eV and 1.15eV as a function of 1 sun illumination time (left axis) and ESR bulk spin density (right axis) as a function of 1 sun illumination time.

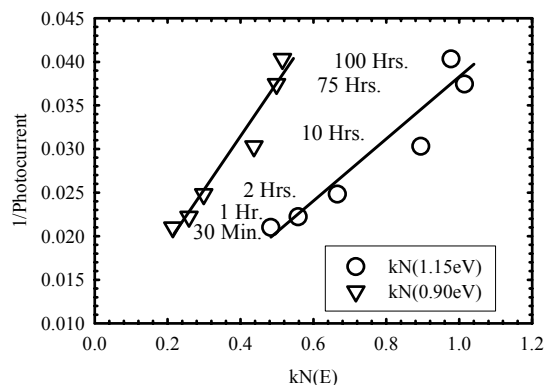


Fig. 4.5 $1/\text{photocurrent}$ plotted as a function of $kN(E)$ at 0.90eV and 1.15eV.

A comparison between the evolution of the states centered around 0.9eV and 1.15eV is shown in Fig. 4.4 where, the $kN(E)$ values at these energies (left axis) are plotted as a function of 1 sun illumination time. Also, on the right axis the bulk spin densities measured by ESR are shown after 1, 10, and 100 hour illumination times. Also shown in the figure are the values in the AS. The key features of the $kN(E)$ evolution for both these energies is the very large increase from the AS in the first hour of degradation and much slower subsequent evolution to a DSS. This feature is also reflected in the ESR results. However, the similarity between the evolution of the three results precludes at this time any conclusions being drawn as to which states can be directly related with D^0 . These preliminary results on the $kN(E)$ spectra, nevertheless, are consistent with a fast and slow component/mechanism playing a role in the creation of both defect states.

There have been many results reported in which the electron $\mu\tau$ products have been correlated with the magnitudes of $\alpha(E)$ at around 1.2eV. The linear correlations between $1/\mu\tau$ (1/photocurrent), which reflects the densities of recombination centers, were found to be distinctly different for different a-Si:H films. The correlations obtained between $1/\mu\tau$ for $G = 5 \times 10^{15} \text{cm}^{-3}\text{s}^{-1}$ and the values of $kN(E)$, not $\alpha(E)$, at 0.9 and 1.15eV are shown in Fig. 4.5. From these preliminary results linear relationships can be inferred with slopes which differ by less than a factor of 2, a difference in slopes is similar to those reported between the results with $\alpha(E)$ obtained from different a-Si:H films. From the results in Fig. 4.5, no reliable conclusions can be drawn about the nature of the gap states centered around midgap and 1.15eV. This is complicated not only by the uncertainties in the $kN(E)$ values but also because they are dependent on the electron occupation and not the densities of the states. In addition, further uncertainty is introduced by the assumption that all the gap states have the same matrix elements for electron transitions into the conduction band as well as the overlap in the distributions of the different gap states.

A room temperature recovery is observed in the photocurrents of thin films after degradation with 1 sun illumination at 25°C. This relaxation is consistent with the presence of “fast” states such as have been observed after high illumination intensities and inferred from the temperature dependence of the 1 sun degradation in films and cells. However, it complicates the study of the light induced defects and the kinetics of their creation. Nevertheless, with the limitations present on the $\alpha(E)$ spectra measurements, the evolution of different light induced gap states centered around midgap and around 1.15eV from the conduction band has been characterized. The large increases in $kN(E)$ spectra in the first hour of degradation are found in both the gap state distributions and ESR measurements with subsequently much slower changes to the DSS. The similarity of the kinetics in all three cases obtained here does not allow the D^0 states to be reliably associated with either gap state distribution. From these preliminary results it is also not been possible to draw reliable conclusions about the actual density of states. Additional studies on both films and solar cell structures are being carried out to obtain more detailed and reliable information.

Appendix A
(*Mat. Res. Soc. Symp. Proc.* 808, A8.8.1 (2004))

**CHARACTERIZATION OF THE BULK RECOMBINATION IN HYDROGENATED
AMORPHOUS SILICON SOLAR CELLS**

J. Deng, J.M. Pearce, V. Vlahos, R.W. Collins, and C.R. Wronski

Center for Thin Film Devices, the Pennsylvania State University, University Park, PA 16802

ABSTRACT

Dark forward bias current, J_D -V, characteristics offer a probe for characterizing carrier recombination and the defect states in the intrinsic layers of hydrogenated amorphous silicon (a-Si:H) solar cells. Detailed studies were carried out on such characteristics for the cells with optimized p/i interfaces and high quality i-layers in which the current transport is bulk recombination dominated. It was found that the diode quality factor n is not a constant with bias voltages as has been generally considered. Instead, it can be best described through the bias dependent differential diode quality factors, $n(V) = [kT/q]^{-1} [d(\ln J_D)/dV]^{-1}$, whose magnitude and shape reflect the gap state distribution in the corresponding bulk i-layers. The $n(V)$ characteristics obtained on cell structures with both hydrogen diluted and undiluted i-layers have been utilized in characterizing the differences in the distribution of defect states in the two i-layers both in annealed state as well as after creating light induced defects. In the characterization of the Staebler-Wronski Effect (SWE) using J_D -V characteristics, a new phenomenon is observed – relaxation of light induced defect states created by 1 sun illumination at 25°C, which is also found in the follow-on studies on the photo-conductivities of corresponding thin films.

INTRODUCTION

Previous studies have shown that it is possible in forward bias current-voltage (J_D -V) characteristics of a-Si:H p-i-n and n-i-p solar cells to separate the carrier recombination in the bulk of the i-layers from that in the p/i interface regions [1-4]. In cell structures having appropriate protocrystalline a-Si:H interface regions bulk recombination dominates the characteristics over a wide range of voltage. Results have also been obtained which clearly establish the absence of the high densities of defect states at the p/i, n/i interfaces predicted by the defect pool model [3]. The absence of such highly non-uniform distributions of gap states across the i-layer reduces the large complexity in the interpretation of J_D -V characteristics in terms of carrier recombination and gap states in the i-layers and allows them to be addressed with an analysis based on first principles [5]. In this treatment account is taken of (i) the homogenous densities of defect states across the entire i-layer; (ii) the potential barriers V_n , V_p adjacent to the n, p contacts due to the high concentration of carriers there and (iii) Shockley-Reed-Hall (SRH) diffusion/recombination in the bulk and at the p/i interfaces. As a consequence the contribution to the currents of recombination in the bulk is most pronounced at low biases with those of the p/i interface at the higher voltages. As the voltages approach the built-in potential, V_{bi} , the currents become limited by carrier injection over the potential barriers V_n , V_p

[6]. Generally the J_D -V characteristics of a-Si:H cells are characterized as in the case of crystalline materials, with a constant diode quality factor n [7-10]. For purely p/i interface recombination currents n has values close to 1 and for currents limited by carrier injection values of n can be greater than 2. Because of the continuous distribution of gap states, currents that are completely dominated by bulk recombination on the other hand have “effective” n values that lie between 1 and 2.

It should be pointed out here that depending on the relative magnitudes of bulk and p/i interface recombination “effective” n values between 1 and 2 are still obtained so that great care must be taken in establishing that the contribution is solely due to the bulk. Such bulk recombination through a continuous distribution of gap states does not result in n values that are independent of voltage except in the special case of an exponential distribution around midgap [8]. Since this is not generally the case, the diode quality factors are not constant with voltages but can be best represented by a “differential diode quality factors $n(V)$ ” which are defined as the inverse of $[kT/q][d(\ln J_D)/dV]$. From this definition, the value of $n(V)$ thus depends on the rate of increase in the current with voltage. Since the recombination currents are determined by the total defects lying between the two quasi-Fermi levels [11], the distance between which is equal to the applied voltage, the values of $n(V)$ reflect the rate of increase in the gap states densities as the quasi-Fermi levels sweep through the energy gap.

Reported here is a study of forward bias dark currents in which bulk recombination is clearly established and then characterized prior to and after introducing light induced defects. The corresponding $n(V)$ characteristics for the annealed and degraded protocrystalline (diluted) and undiluted a-Si:H are then presented and discussed in terms of their respective distributions of gap states. Results are also presented on the observation of a new phenomenon in SWE – the thermal relaxation of defect states at room temperature created by 1 sun illumination.

EXPERIMENTAL DETAILS

The p (a-SiC:H)/ i (a-Si:H)/ n (μ c-Si) (superstrate) a-Si:H solar cells studied here were fabricated by RF plasma enhanced chemical vapor deposition at a substrate temperature of 200°C under conditions described previously [1]. The i-layers in the cell structures were deposited using SiH_4 diluted with H_2 , with $R = [\text{H}_2]/[\text{SiH}_4]$ of either 10 (diluted) or 0 (undiluted). To minimize the contributions of shunts, cell structure areas of 0.02 cm² were used, which were defined by removing the top n μ c-Si:H layers with reactive ion etching. The J_D -V characteristics measurements were carried out at temperatures which were controlled to $\pm 0.1^\circ\text{C}$ and a three-probe technique was used to eliminate any extraneous series resistance effects. Care was taken to ensure that the steady-state currents were measured at low biases and that no defects were introduced by double injection in the high forward bias regions. Annealed state is achieved by heating the cells for 4 hours at 170°C and the SWE defects are introduced using illumination generated by ELH lamp which has light intensity equivalent to that of 1 sun illumination.

RESULTS AND DISCUSSION

Differential Diode Quality Factor $n(V)$

Highly reproducible J_D -V characteristics were obtained on these 0.02 cm² cell structures over extended regions of voltage apart from occasional contributions of shunts at the lowest

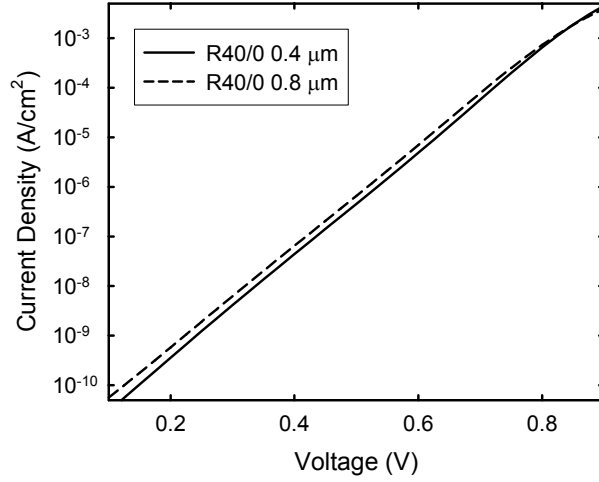


Figure 1: J_D - V characteristics of p-i-n cell structures with 0.4 and 0.8 μm thick undiluted ($R=0$) a-Si:H i-layers and 200 \AA thick $R=40$ a-Si:H p/i interface layer in their annealed state.

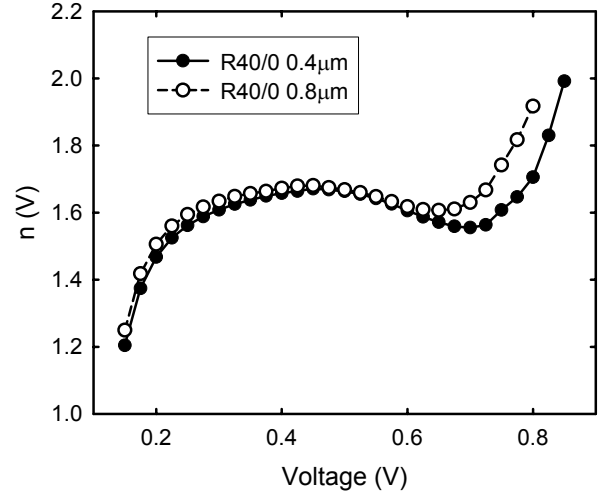


Figure 2: $n(V)$ characteristics obtained for p-i-n cell structures of Figure 1.

biases ($<0.2\text{V}$). In Figure 1 the J_D - V characteristics are shown for two p-i-n cell structures with 0.4 and 0.8 μm thick undiluted ($R=0$) a-Si:H i-layers and 200 \AA thick $R=40$ a-Si:H p/i interface layer in their annealed state. It can be seen in the figure that there is a clear i-layer thickness dependence of J_D - V characteristics over the voltage range 0.1 \sim 0.7V. Since the changes in J_D - V characteristics from cell to cell on the 6 cm^2 sample and between different samples are within $\sim 10\%$, they allow the bulk recombination to be reliably characterized for these two thicknesses. The scaling of the currents with i-layer thickness, a factor of ~ 1.5 rather than 2, can be attributed to the non-uniform electric field distribution across the i-layer due to the space charge present there [3].

The $n(V)$ characteristics for the cell structures of Figure 1 are shown in Figure 2. They not only exhibit a clear bias dependence but also excellent overlap between them from below 0.2V to around 0.6V. This is consistent with the fact that the $n(V)$ characteristics at these voltages reflect the gap state distribution in the i-layer and thus are independent of their thickness. At the low voltages around 0.2V, where only defects around midgap are involved in the recombination, there is a rapid increase in $n(V)$ indicating that as the quasi-Fermi level splitting increases the gap states involved in the recombination hardly change. This suggests that there may exist a Gaussian-like distribution of gap states centered around the midgap so that the defect density decreases rapidly with energy away from midgap. At voltages between 0.3V and 0.6V, the $n(V)$ values are approximately constant (~ 1.6), indicating the onset of an exponential-like distribution of defects further away from midgap. At the highest voltages the characteristics separate where the $n(V)$ values start to increase rapidly and eventually become larger than 2. This reflects the currents becoming carrier injection limited at these voltages and is consistent with the results obtained from the studies on J_D - V characteristics [3, 5].

Since the $n(V)$ characteristics reflect the gap state distributions, they can be utilized in characterizing the distributions in the different i-layers incorporated into cell structures. Shown in Figure 3 are the $n(V)$ characteristics for cells in their annealed state with 0.4 μm thick $R=10$ and $R=0$ bulk i-layers in which the p/i recombination is minimized by having a 200 \AA $R=40$ i-layer at p/i interface. It can be seen from Figure 3 that, as in the case of $R=0$, $n(V)$ for the cell

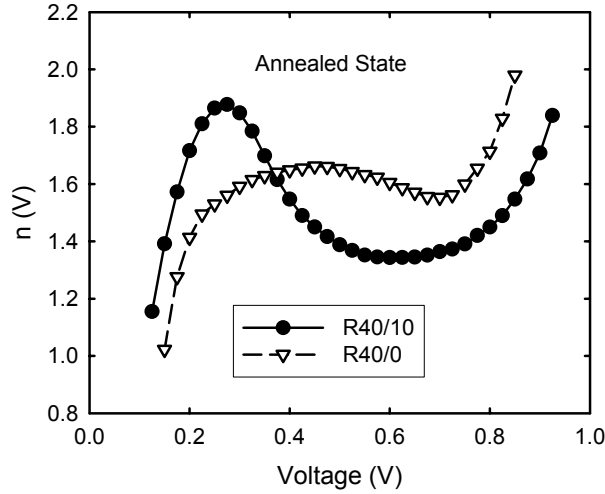


Figure 3: $n(V)$ characteristics of p-i-n cell structures with $0.4\mu\text{m}$ thick $R=0$ and $R=10$ a-Si:H i-layers and 200\AA thick $R=40$ a-Si:H p/i interface layer at their annealed state.

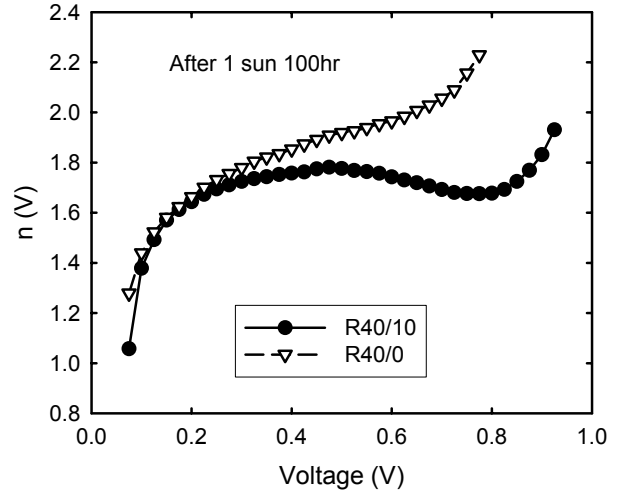


Figure 4: $n(V)$ characteristics obtained for p-i-n cell structures of Figure 3 after 100 hr of 1 sun illumination.

with $R=10$ bulk i-layer also exhibits a rapid increase at voltage smaller than about 0.2V . This indicates the presence of a Gaussian-like distribution centered around midgap in $R=10$ i-layer, similar to the case of the $R=0$ i-layer whose magnitude and width are somewhat different. For voltages larger than 0.25V , $n(V)$ decreases rapidly to an approximately constant value of ~ 1.4 that is smaller than in the cell with the $R=0$ i-layer. This indicates that the increase with energy of this exponential-like gap state distribution is faster in the $R=10$ than that in the $R=0$ i-layer. It can also be seen in Figure 3 that the $n(V)$ values become larger than 2 at a lower voltage for the cell with $R=0$ i-layer. This is consistent with the fact that the currents in this cell become carrier injection limited at a lower voltage due to the higher recombination currents in large part because of the lower bandgap in the $R=0$ material. Although detailed and more elaborate analysis is needed for obtaining exact distributions of the gap states, these results clearly indicate that the distributions in the $R=0$ and $R=10$ materials in their annealed state are distinctly different.

A distinct difference in the distribution of light induced gap states in the two materials is also indicated from $n(V)$ characteristics. The results obtained 24 hours after exposing the cells of Figure 3 for 100 hours of 1 sun illumination at 25°C are shown in Figure 4. Based on a similar analysis as above it can be seen that in the case of the $R=10$ material there is still a Gaussian-like distribution around midgap followed by an exponential-like gap state distribution. The higher approximately-constant $n(V)$ value of ~ 1.7 at voltages between 0.2 and 0.8V in the $R=10$ cell, however, indicates that the exponential-like distribution increases with energy at a smaller rate compared to the annealed state as a result of light induced defects. On the other hand, in the cell with $R=0$ i-layer, $n(V)$ increases monotonically with bias over the entire voltage range. This is an indication that in this case the resultant defect states have the highest density around midgap which now gradually decreases at energies further away from midgap.

Room Temperature Annealing of Light Induced Defects

In the course of investigating the J_D - V characteristics after 1 sun illumination at 25°C the relaxation was observed in their light induced changes. This relaxation, which occurs in cells

having both $R=10$ and $R=0$ i-layers, is readily observed at the low forward biases where the currents are determined by recombination in the bulk of the i-layers. This is illustrated in Figure 5 with the changes in J_D -V characteristics that occur in 50 hours in the $R=10$ cell of Figure 3 after it has been degraded for 30 minutes with 1 sun illumination at 25°C . The figure shows the increase after the illumination and the subsequent decrease/relaxation of the currents over the voltage range where they are dominated by bulk recombination. In Figure 6 the relaxation in the recombination currents, normalized to their respective initial values immediately after illumination, is shown for the three voltages corresponding to quasi-Fermi level splitting of 0.3eV , 0.4eV and 0.5eV . It can be clearly seen in the figure that very large changes occur in the recombination through the states within 0.3eV of midgap where there is a decrease of $\sim 40\%$ in 100 minutes. It can also be seen that as the separation between the quasi-Fermi levels becomes larger there is a systematic decrease in the relaxation. Under these conditions two things occur: gap states further away from midgap are introduced into the recombination process and the recombination currents themselves increase which can enhance the erasure of the relaxation.

The results obtained on the large relaxation of light induced defect states close to midgap at room temperature are highly significant. They introduce even more complexity into the nature of the light induced defects but may offer some additional insight in addressing the mechanisms responsible for creating SWE defects. That the changes found here in light induced defects at midgap are so large maybe somewhat surprising. However it is not so surprising that they have not been observed/ reported previously in the extensive studies carried out on either cells or films because they can be readily detected and characterized only in the presence of small quasi-Fermi level splitting and low carrier recombination.

CONCLUSIONS

The results presented and discussed here demonstrate that dark forward bias J_D -V characteristics offer a new and powerful probe for the study of defect states in the i-layers of

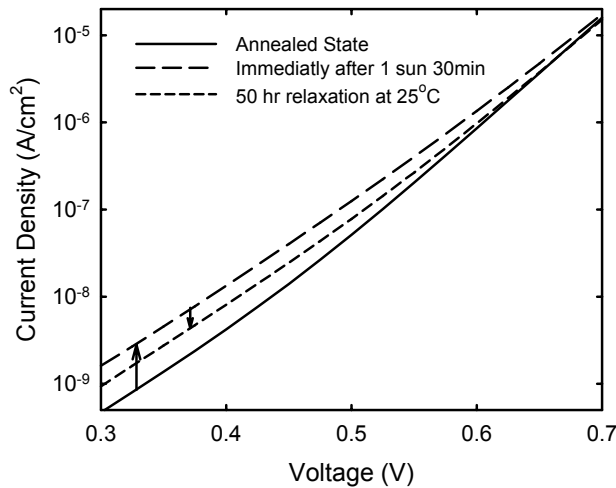


Figure 5: Degradation and subsequent relaxation of dark current at room temperature for the cell of Figure 3 with $R=10$ bulk i-layer.

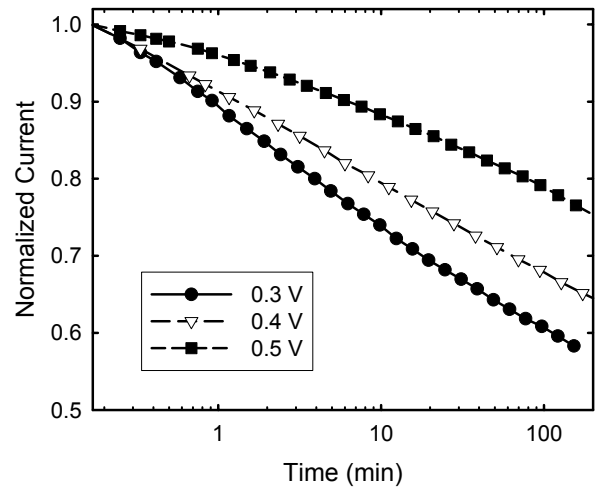


Figure 6: Degradation and subsequent room temperature relaxation of dark current at fixed monitoring voltages for the cell of Figure 5.

a-Si:H solar cells providing bulk recombination can be clearly established. This ability has allowed the first direct observation of thermal relaxation in the light induced defect states created by 1 sun illumination at 25°C. Such relaxation, which is readily observed in the recombination currents at low forward biases, is indicative of the “fast” states that have been observed in the studies using high intensity illumination [12]. This relaxation has subsequently been observed in very careful studies of photo-conductivities in corresponding a-Si:H films. The results presented on the differential diode quality factors, $n(V)$, for J_D -V characteristics corresponding to recombination in the bulk of the i-layers are shown to be consistent with homogenous distribution of defects having a continuous distribution of gap states across the gap. From the results obtained on cells with diluted, $R=10$, and undiluted, $R=0$, i-layers it was possible to identify the distinct differences in their densities of states both for the annealed as well as after degradation with 1 sun illumination.

ACKNOWLEDGEMENT

We would like to acknowledge P. C. Taylor and B. von Roedern for helpful discussions. This research was supported by the National Renewable Energy Laboratory under subcontract NDJ-2-30630-01.

REFERENCES

- [1] R. J. Koval, J. Koh, Z. Lu, L. Jiao, R. W. Collins, and C. R. Wronski, *Appl. Phys. Lett.* **75**, 1553 (1999)
- [2] J. M. Pearce, R.J. Koval, A.S. Ferlauto, R.W. Collins, C. R. Wronski, J. Yang, and S. Guha, *Appl. Phys. Lett.* **77**, 3093 (2000)
- [3] J. Deng, J. M. Pearce, R. J. Koval, V. Vlahos, R.W. Collins, and C. R. Wronski, *Appl. Phys. Lett.* **82**, 3023 (2003)
- [4] V. Vlahos, J. Deng, J. M. Pearce, R. J. Koval, R. W. Collins and C. R. Wronski, *Mat. Res. Soc. Proc.* **762**, A7.2 (2003)
- [5] C. R. Wronski, R. W. Collins, V. Vlahos, J. M. Pearce, J. Deng, M. Albert, G. M. Ferreira, and C. Chen, “Optimization of Phase-Engineered a-Si:H-Based Multijunction Solar Cells”, *National Renewable Energy Laboratory Annual Report*, Contract #: NDJ-2-30630-01, (2004)
- [6] J. Deng, J. M. Pearce, V. Vlahos, R. W. Collins, and C. R. Wronski, *Mat. Res. Soc. Proc.* **762**, A3.4 (2003)
- [7] H. Sakai, T. Yoshida, S. Fujikake, T. Hama, and Y. Ichikawa, *J. Appl. Phys.* **67**, 3494 (1990)
- [8] C. van Berkel, M. J. Powell, A. R. Franklin, and I. D. French, *J. Appl. Phys.* **73**, 5264 (1993)
- [9] M. A. Kroon and R. A. C. M. M. van Swaaij, *J. Appl. Phys.* **90**, 994 (2001)
- [10] K. Lord, B. Yan, J. Yang, and S. Guha, *Appl. Phys. Lett.* **79**, 3800 (2001)
- [11] A. Rose, “Concepts in Photoconductivity and Allied Problems”, Interscience, New York, 1962
- [12] J. M. Pearce, R. J. Koval, X. Niu, S. J. May, R. W. Collins, and C. R. Wronski, *17th European Photovoltaic Solar Energy Conference Proceedings*, **3**, 2842 (2002)